Longitudinal dispersion in a partially mixed estuary

by Robert E. Wilson[1] and Akira Okubo[1]

ABSTRACT

Within a partially mixed estuary both the tidal and the nontidal density-induced circulation exhibits substantial vertical shear. The interaction of this current shear with turbulent mixing across the vertical density gradient contributes to the longitudinal (alongstream) spread of a contaminant introduced into the estuary. A dye tracer experiment conducted in the lower York River Estuary provides abundant evidence for the importance of this "shear effect" to longitudinal dispersion. We have documented the vertical movement of dye, the longitudinal movement of the center of mass, and the longitudinal spread as represented by the variance of the distribution following a point source release. We have presented a shear-diffusion model which describes the vertical distribution of dye as a function of time, and the asymptotic behavior of both the first and second moments of the longitudinal distribution for times very short and very long compared to the time of vertical mixing within the estuary. The model includes the effects associated with nontidal upward advection.

1. Introduction

This paper presents an analysis of experimental results from a dye tracer experiment conducted in the lower reaches of the York River estuary during October of 1960. The experiment involved an instantaneous release of dye at depth within the estuary. Concentrations of dye were then monitored for up to 100 hours following the release. The objectives of the experiment were to obtain information on the intensity of contaminant dispersion in the specific location (Fig. 1) and, more generally, to examine the characteristics of dispersion in a stratified estuary.

The York River is a tributary estuary of the Chesapeake Bay. As shown in Figure 2, it exhibits moderate stratification over its lower reaches with increasing stratification downstream. Flow patterns within the York are characteristic of those for a partially mixed estuary as described by Pritchard (1955). In this type of estuary, considerable vertical mixing occurs across the vertical density gradient which is maintained by a net nontidal circulation involving downestuary flow in the surface layers and upestuary flow at depth. There is also a small net vertical motion directed from the deeper layers to the surface layers. Superimposed on this nontidal

1. Marine Sciences Research Center, State University of New York, Stony Brook, New York, 11794, U.S.A.

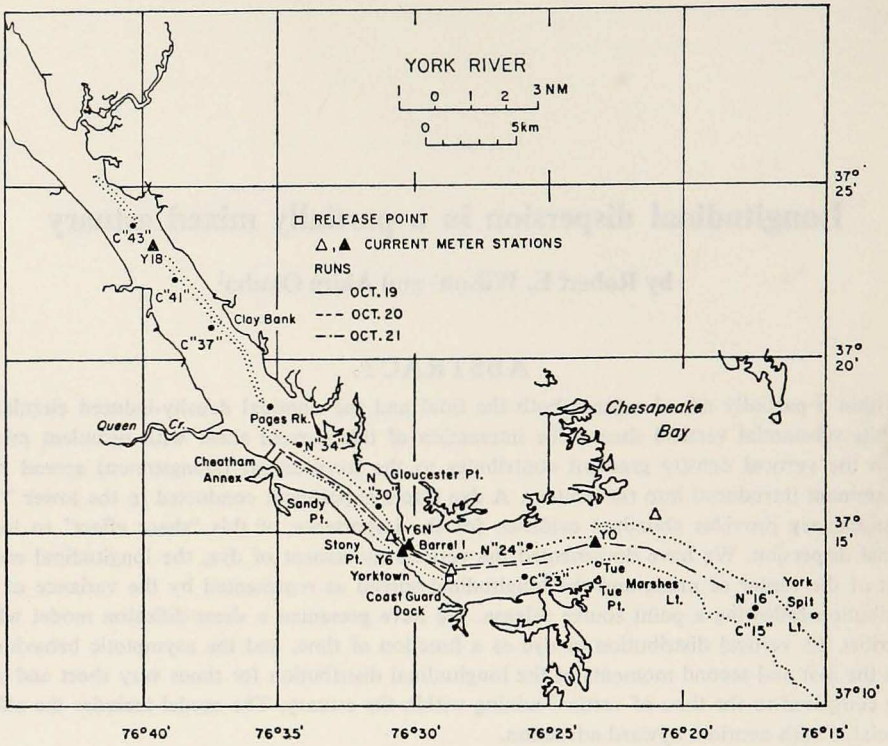

Figure 1. The York River Estuary. Shown are the positions of the dye tracer release, the hydrographic and current meter stations, and the lateral and longitudinal observational runs.

flow is a strong oscillatory tidal motion. In the lower reaches of the York River characteristic velocities for the nontidal horizontal flow range from 5 to 10 cm s^{-1} (Fig. 3), and tidal current amplitudes range from 60 to 100 cm s^{-1} (Fig. 4).

The interaction of vertical mixing with vertical shear in both the horizontal tidal and nontidal currents contributes to the spread of an introduced substance in the direction of the flow. The importance of this "shear effect" to dispersion in general, and to longitudinal dispersion in estuaries in particular (Bowden, 1965), has been realized for some time. In this paper we have studied longitudinal dispersion in the York River in light of the theoretical techniques and results presented by Okubo (1967, 1968) by examining the time history of the first few moments associated with the longitudinal distribution of dye.

2. A description of the dye tracer experiment

Figure 1 presents a map of the specific area in which the dye tracer experiment was conducted. It shows the location of the dye release, the 5 fathom depth contour,

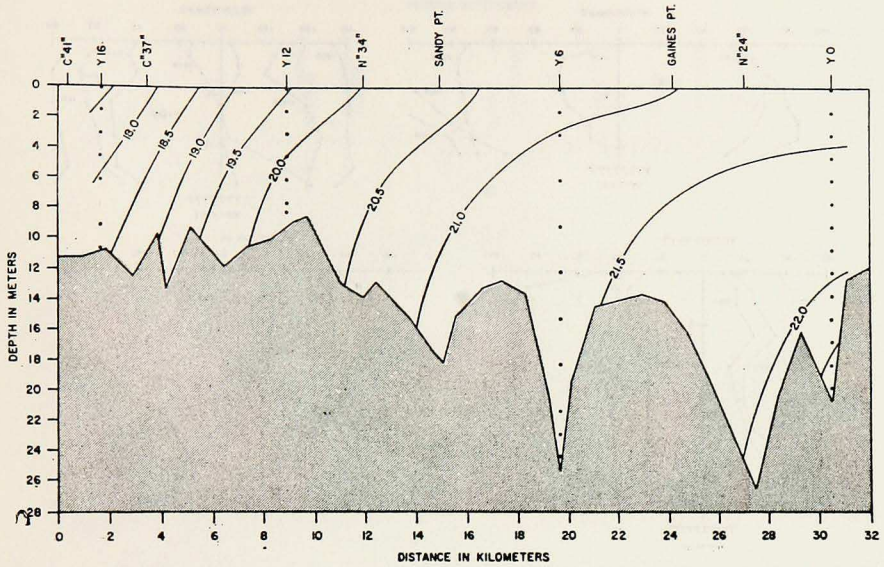

Figure 2. Salinity section in the lower York River on the slack before flood, 30 July, 1954.

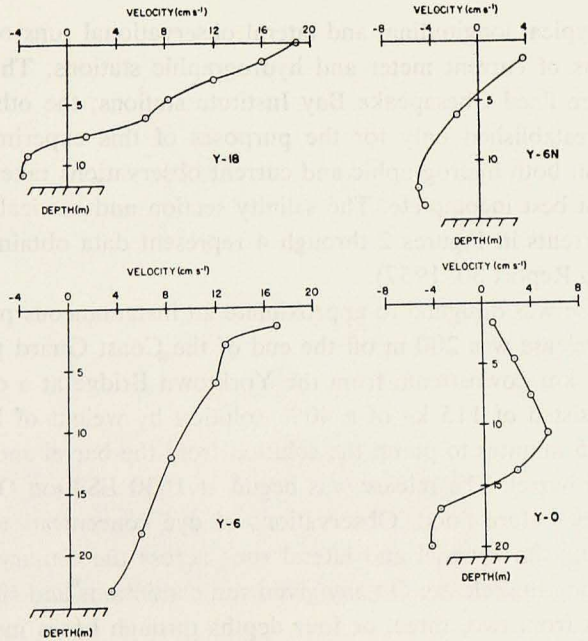

Figure 3. Nontidal longitudinal currents computed from 25 hours of current observations at each station during the period 29 July-1 August, 1954.

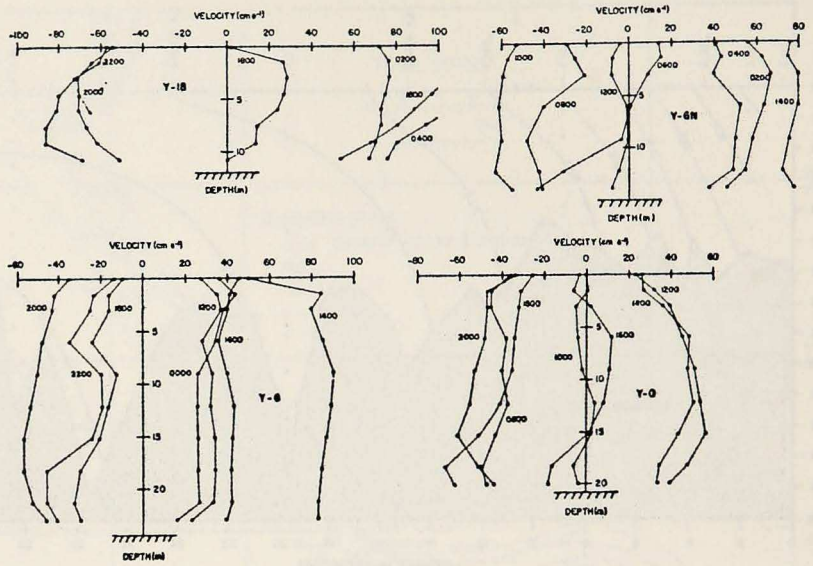

Figure 4. Longitudinal currents at two-hour intervals throughout the tidal cycle. Times are EST. Dates of observations are: Y-0, 29 July, 1954; Y-6, 30 July, 1954; Y-6N, 31 July, 1954; Y-18, 31 July, 1954.

the position of typical longitudinal and lateral observational runs on different days, and the positions of current meter and hydrographic stations. The stations designated by "Y" are fixed Chesapeake Bay Institute stations; the other stations were temporary and established only for the purposes of this experiment. We should mention here that both hydrographic and current observations taken during this experiment were at best incomplete. The salinity section and vertical profiles of tidal and nontidal currents in Figures 2 through 4 represent data obtained on an earlier cruise (CBI Data Report 30, 1957).

The dye release was designed to approximate an instantaneous point source. The position of the release was 200 m off the end of the Coast Guard pier (Fig. 1) and approximately 4 km downstream from the Yorktown Bridge at a depth of 10.5 m. The release consisted of 115 kg of a 40% solution by weight of Rhodamine B in alcohol; it took 5 minutes to pump the solution from the barrel and another 5 minutes to rinse the barrel. The release was begun at 1630 EST on October 18, 1960 on the tidal slack before flood. Observations of dye concentration involved longitudinal runs along the channel and lateral runs across the estuary for a period of four days following the release. On any given run continuous and simultaneous samples were drawn from two, three, or four depths through hoses inside a suspended strut. Separate fluorometers measured dye concentrations for each depth.

As shown in Figure 4, the amplitude of tidal currents within the reach is of the

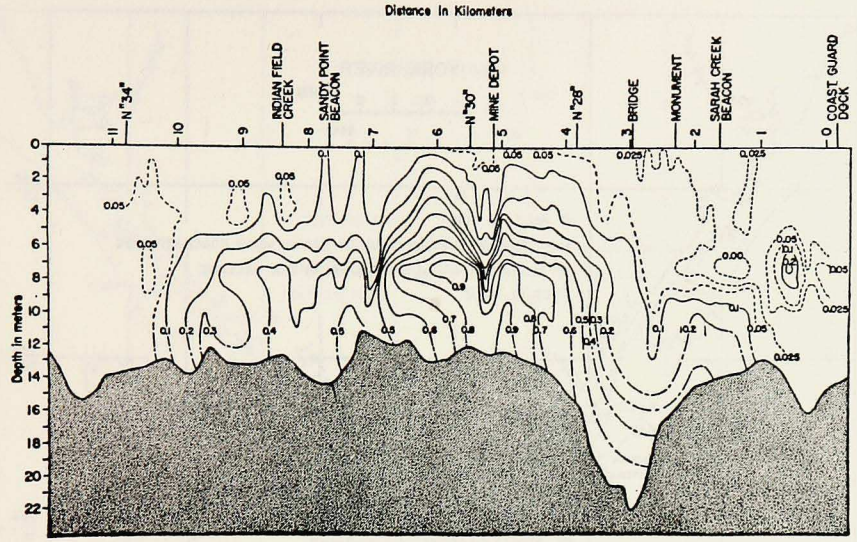

Figure 5. Longitudinal section of dye concentration for Run 1, 0824-0923 EST, 19 October, 1960. Section was traversed from Coast Guard Dock to N"34" during a flooding tide; maximum flood was at 0650 EST. Dye concentrations are in parts per billion.

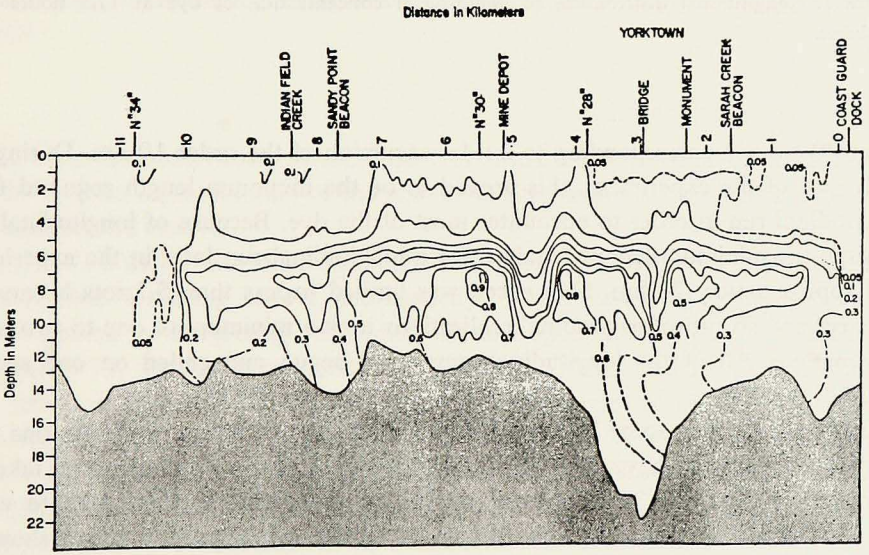

Figure 6. Longitudinal section of dye concentration for Run 2, 0954-1125 EST, 19 October, 1960. Section was traversed from N"34" to Coast Guard Dock during an ebbing tide; maximum ebb was at 1310 EST. Dye concentrations are in parts per billion.

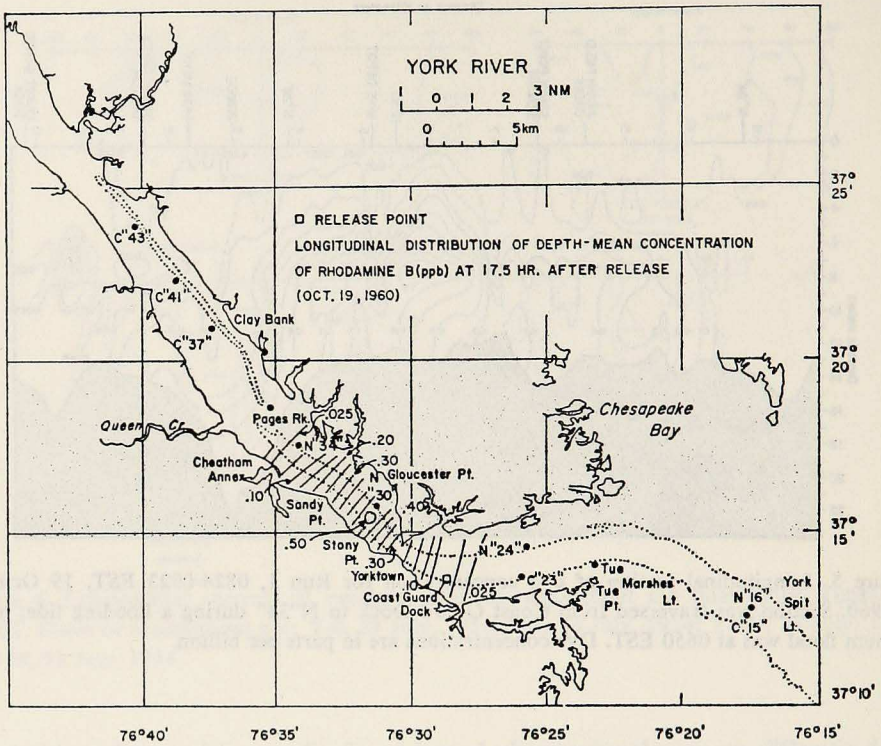

Figure 7. Longitudinal distribution of depth-mean concentration of dye at 17.5 hours after release.

order 80 cm s^{-1} corresponding to a tidal excursion of the order 10 km. During the early part of the experiment, this proved to be the minimum length required for a longitudinal run in order to encounter most of the dye. Because of longitudinal dispersion, the minimum length required for a longitudinal run later in the experiment was approximately 20 km. Ship speed was limited to less than 5 knots because of the strut and so entire longitudinal realizations took a minimum of one to two hours to complete. All of the longitudinal runs were begun and ended on one specific phase of the tide.

In order to obtain some idea of how representative these observational runs were of synoptic data, we have compared the distributions from duplicate runs taken in immediate succession. This, at least, provides information on the extent to which the distribution has changed over the period of the run. Figures 5 and 6 show the distributions from the duplicate runs. The distribution from the second run shows more dispersion, but there is striking similarity between the two distributions. This suggests that the time scale for significant change in the distribution is considerably

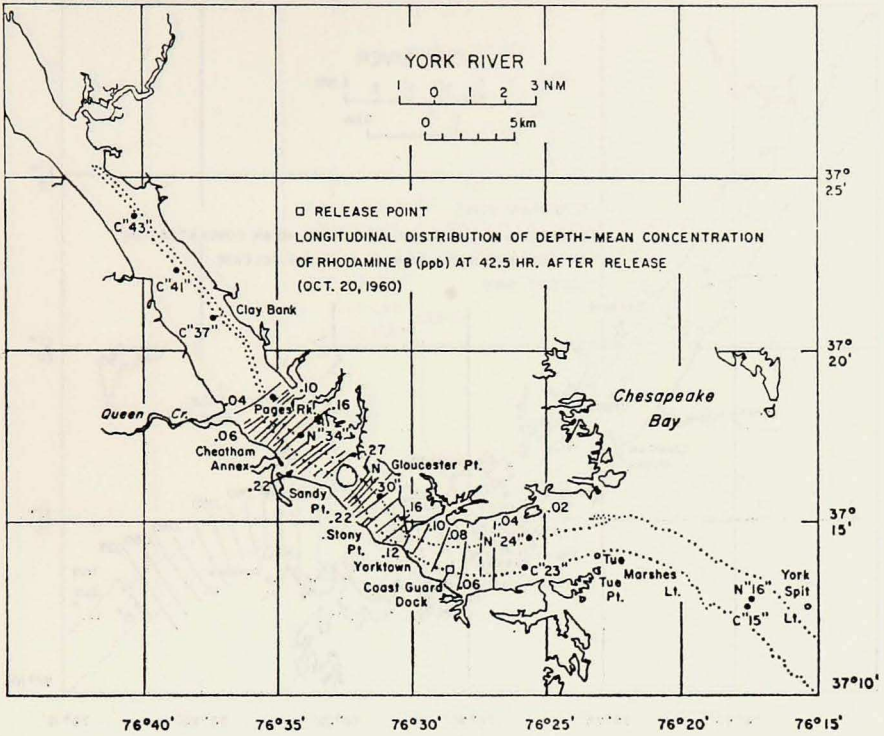

Figure 8. Longitudinal distribution of depth-mean concentration of dye at 42.5 hours after release.

greater than the observation period, and that distribution realized on a given run provides a good representation of the instantaneous pattern at the centered time of the observational interval.

Figures 7, 8 and 9 are maps showing the horizontal distribution of depth-mean concentration, assuming lateral homogeneity. These depth-mean concentrations were computed by integrating concentrations at a specific axial position vertically. On October 19, the depths sampled were 1.5, 4.5, 7.5 and 10.5 m. The concentrations shown in Figure 7 for the 19th represent the geometric mean of the depth-mean concentrations from duplicate observations. The only depths sampled on October 20 were 6 and 10.5 m because the distribution was approaching vertical homogeneity. The depth-mean concentrations for this run are represented by a straight average of concentrations at 6 and 10.5 m. On October 22, the depths sampled were 1.5, 6.0 and 10.5 m. It is apparent from these figures that the original patch of dye has undergone considerable longitudinal dispersion, even on the first day after the release. The distributions shown in Figures 8 and 9 are skewed down-

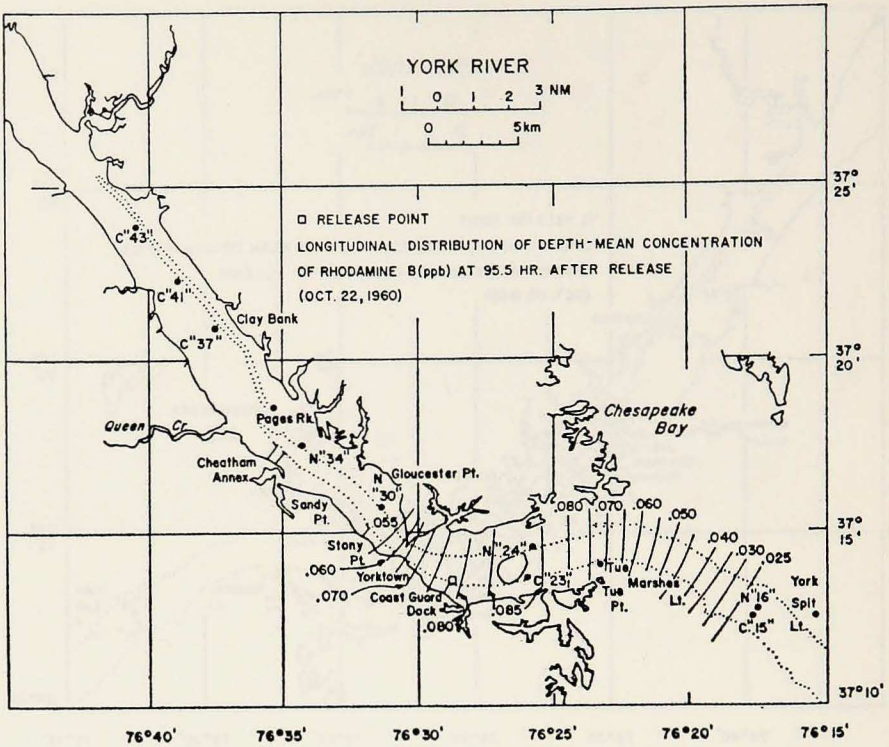

Figure 9. Longitudinal distribution of depth-mean concentration of dye at 95.5 hours after release.

estuary. This type of skewed distribution is frequently encountered in estuarine diffusion and may be attributed primarily to the increasing power of diffusion downstream (Kent, 1960).

Figure 10 shows the horizontal distribution of dye at 1.5 and 10.5 m on October 22. The upestuary shift of the distribution at depth relative to that in the upper layers is obvious. This is the pattern we would expect for nontidal circulation with upestuary flow at depth and downestuary flow in the surface layers. Given this type of sheared pattern of dye, it is clear how vertical mixing interacts with a vertical shear in horizontal current to accelerate longitudinal dispersion.

Plotted in Figures 11, 12 and 13 is dye concentration versus longitudinal distance for the distributions represented in Figures 7 through 10. We have computed the center of mass, the standard deviation, and the variance for each of the distributions of depth-mean concentration (Table 1). We will compare the observed time rate of change of the variance to theory later.

The experiment included a number of successive observations of the distribution of dye (Fig. 14) in a fixed cross section from the Coast Guard Pier to Barrel "1".

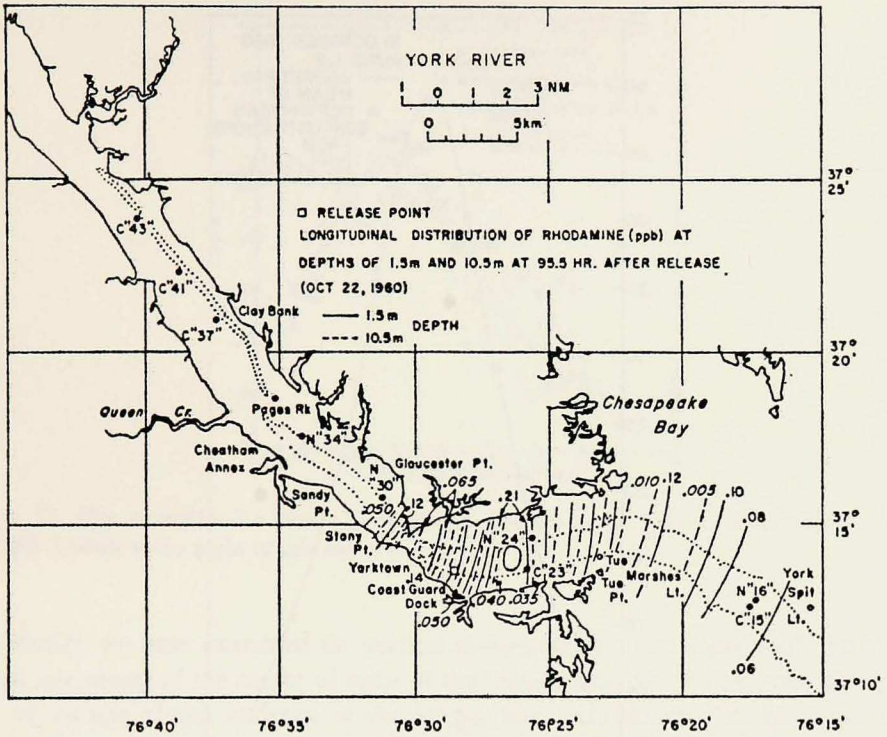

Figure 10. Longitudinal distribution of dye concentration at depths of 1.5 m and 10.5 m at 95.5 hours after release.

The purpose of these observations was to provide information on the time history of the lateral and especially the vertical structure of dye concentration. In spite of the fact that this section did not always cut the dye distribution at a unique position, such as the center of mass, it was frequently close to this position. These sections should, in any case, supply information on the relative vertical and lateral structure as a function of time.

The sections show that the dye was initially concentrated in the vicinity of the

Table 1. Characteristics of the longitudinal distribution of dye. The origin of the x coordinate is taken as the point of release; x is positive downestuary.

Time after release t (hr)	Centroid of the distribution $\bar{x}$ (km)	Standard deviation σ_x (km)	Variance σ_x^2 (km^2)
17.5	−5.3	2.5	6.1
42.5	−6.8	4.7	22.0
95.5	3.2	8.3	68.5

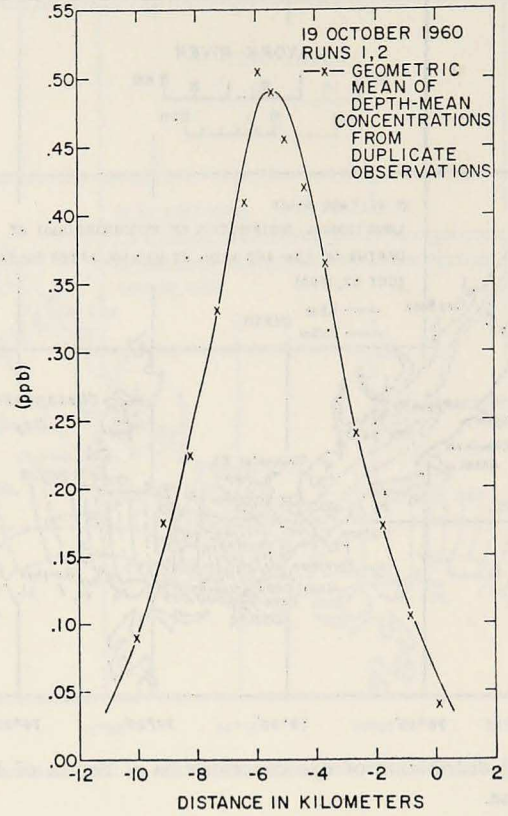

Figure 11. Dye concentration versus longitudinal distance at 17.5 hours after release. The origin is taken as the point of release.

depth of release at 10.5 m. The dye then diffused vertically as though the apparent upward diffusion were faster than the downward diffusion. Eventually dye concentrations in the upper layer exceeded the concentrations at depth. It is possible to explain this net upward movement of dye in terms of the small net upward advection flow characteristic of a partially mixed estuary.

Lateral homogeneity seems to be reasonably well established by the second day after the release. There is, however, some evidence that concentrations tend to be higher on the north side of the section. This is possibly due to lateral circulation effects associated with flow around a bend.

3. Theoretical discussion

We present the following analyses with the objective of providing some insight into the processes which contribute to movement and dispersion just described.

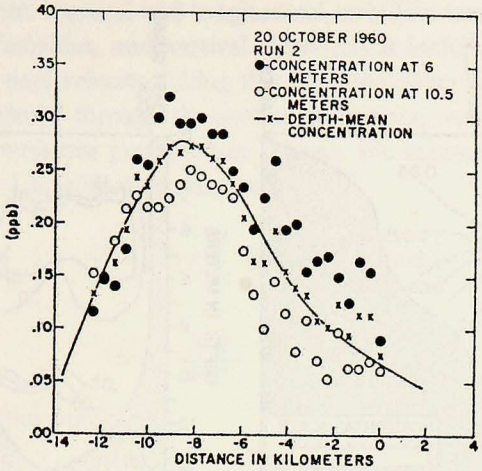

Figure 12. Dye concentration versus longitudinal distance at 42.5 hours after release. The origin is taken as the point of release.

Specifically, we have examined the vertical movement of a tracer material, the horizontal movement of the center of mass of the longitudinal distribution, and the time rate of change of the variance of the longitudinal distribution. We have not addressed the problem of asymmetric diffusion due to longitudinal variations in eddy diffusivity and estuarine cross section.

In light of what we know about the hydrography of the York River, and in light of the observed distributions of dye tracer presented in the previous section, our main emphasis has been in representing the effect of vertical shear in horizontal

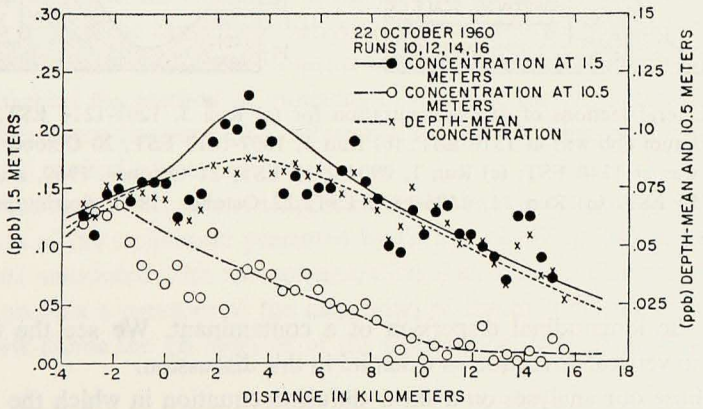

Figure 13. Dye concentration versus longitudinal distance at 95.5 hours after release. The origin is taken as the point of release.

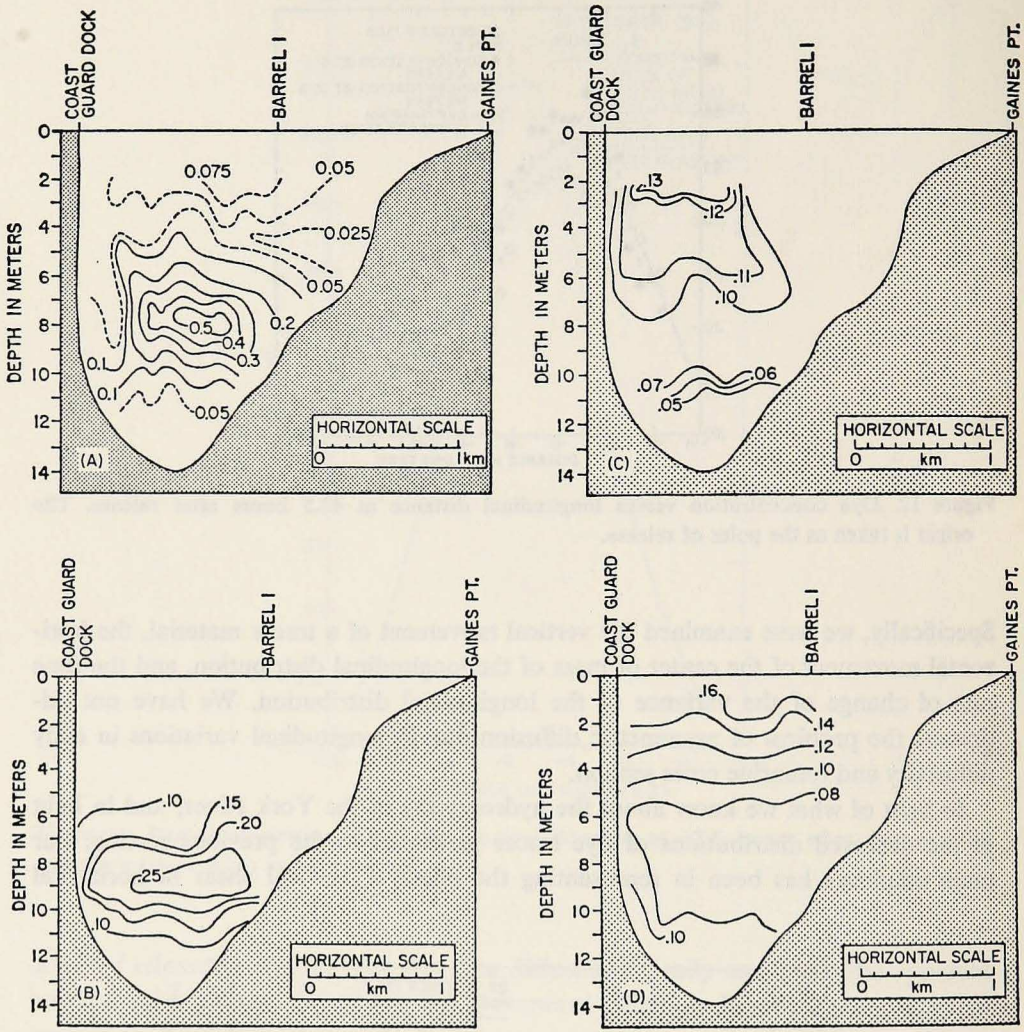

Figure 14. Lateral sections of dye concentration for (a) Run 3, 1207-1214 EST, 19 October, 1960, maximum ebb was at 1310 EST; (b) Run 3, 1607-1617 EST, 20 October, 1960, maximum ebb was at 1340 EST; (c) Run 1, 0904-0915 EST, 21 October, 1960, maximum flood was at 0750 EST; (d) Run 11, 1506-1512 EST, 22 October, 1960, maximum ebb was at 1530 EST.

current on the longitudinal dispersion of a contaminant. We see the inclusion of effects due to vertical advection as essential in this discussion.

We will base our analyses on a shear-diffusion equation in which the longitudinal velocity consists of a nontidal and an oscillatory tidal current, both having uniform vertical gradients. All lateral variations are assumed to be unimportant, and the depth

is taken to be a constant. Vertical and longitudinal turbulent transports are described by constant eddy diffusivities, and vertical advection is included with the assumption of a constant vertical velocity. Using this equation along with boundary conditions of no flux of material through the surface or bottom, we will consider the distribution for an instantaneous point source release. We assume that the concentration of material $S(t,x,z)$ satisfies the equation:

$$\frac{\partial S}{\partial t} + \left[v_1 \left(1 - \frac{z}{d} \right) + v_2 \left(1 - \frac{z}{h} \right) \sin\sigma t \right] \frac{\partial S}{\partial x} + w \frac{\partial S}{\partial z} = K_x \frac{\partial^2 S}{\partial x^2} + K_z \frac{\partial^2 S}{\partial z^2} \tag{1}$$

with boundary and initial conditions:

$$wS - K_z \frac{\partial S}{\partial z} = 0 \qquad z = 0; H \tag{2}$$

$$S(t,x,z) = Q\delta(x)\,\delta(z - z_0) \qquad t = 0. \tag{3}$$

In equations (1)-(3) $S(t,x,z)$ denotes the lateral-mean concentration of material, t is time, x is the longitudinal coordinate, positive seaward with origin at the release point, and z is the vertical coordinate, positive downward with origin at the surface. z_0 is the depth of the release and Q represents the amount of material released per unit lateral length. w is the vertical velocity, positive downward, and K_x and K_z are the longitudinal and vertical eddy diffusivities; all are taken to be constant. v_1 and v_2 are respectively the longitudinal nontidal velocity and the amplitude of the tidal current at the surface; d and h are the length scales for the vertical gradients in nontidal and tidal currents respectively, and σ is the frequency of the tidal current.

This formulation as represented by equations (1)-(3) is similar to that presented by Okubo (1967) with the exception of the term in equation (1) for vertical advection. He determined the asymptotic behavior of the longitudinal (alongstream) variance by calculating the first three moments of the concentration distribution. Okubo (1968) again used the method of moments to examine the asymptotic behavior of longitudinal variance for very long diffusion times for the case of a steady current with shear and vertical advection.

Rather than seek exact or even approximate solutions to equations (1)-(3), we will make use of the techniques presented by Okubo (1967, 1968) to examine certain moments associated with the concentration distribution. The variance in particular will provide a measure of the dispersion of the material about its center of mass. We first define the jth moment of the distribution of material at depth z and at time t:

$$C_j(t,z) = \int_{-\infty}^{+\infty} x^j S(t,x,z)\, dx \qquad (j \geqslant 0). \tag{4}$$

$C_0\ (t,z)$ will then be the total amount of material in a horizontal plane at depth z and at time t. It can then be shown that

$$\bar{x}\ (t) = \frac{1}{Q}\int_0^H dz \int_{-\infty}^{+\infty} x\, S\ (t,x,z)\, dx = \frac{1}{Q}\int_0^H C_1\ (t,z)\, dz \tag{5}$$

$$= \frac{1}{Q}\int_0^t dt' \int_0^H \left[v_1 \left(1 - \frac{z}{d} \right) + v_2 \left(1 - \frac{z}{h} \right) \sin\sigma t \right] C_0\ (t',z)\, dz$$

where $\bar{x}(t)$ represents the position of the center of mass of the entire distribution of material within the estuary. Similarly, the second moment of the entire distribution is

$$\overline{x^2}\ (t) = \frac{1}{Q}\int_0^H dz \int_{-\infty}^{+\infty} x^2 S\ (t,x,z)\, dx = \frac{1}{Q}\int_0^H C_2\ (t,z)\, dz \tag{6}$$

$$= 2K_x t + \frac{2}{Q}\int_0^t dt' \int_0^H \left[v_1 \left(1 - \frac{z}{d} \right) + v_2 \left(1 - \frac{z}{h} \right) \sin\sigma t \right] C_1\ (t',z)\, dz,$$

and the variance of the entire distribution $\sigma_x^2(t)$ may be calculated from

$$\sigma_x^2(t) = \overline{x^2}\ (t) - \bar{x}^2\ (t). \tag{7}$$

Consider first $C_0\ (t,z)$; it must be determined before we can estimate $\bar{x}(t)$ and $\overline{x^2}\ (t)$, but it in itself provides information on the vertical movement of material. The differential equations for $C_0\ (t,z)$ are found by integrating (1)-(3) over all x. The solution for $C_0\ (t,z)$ is

$$C_0\ (t,z) =$$

$$\frac{Q}{H}\left[\frac{\omega}{e^{\omega}-1}\ e^{\omega \frac{z}{H}} + \frac{1}{2}\sum_{m=1}^{\infty} e^{-\left[\frac{\omega^2}{4\pi^2} + m^2 \right] \frac{\pi^2 K_z}{H^2} t + \frac{\omega}{2}\frac{z-z_0}{H}} \right. \tag{8}$$

$$\times \left. \frac{\omega \sin\left(m\pi \frac{z}{H} \right) + 2\pi m \cos\left(m\pi \frac{z_0}{H} \right)}{\frac{\omega^2}{4} + m^2\pi^2} \left[\omega \sin\left(m\pi \frac{z}{H} \right) + 2\pi m \cos\left(m\pi \frac{z}{H} \right) \right] \right]$$

where $\omega = \dfrac{wH}{K_z}$. The solution (8) describes the vertical distribution of a material initially released at z_0 and subject to vertical turbulent mixing and vertical advection. For t very large compared to the vertical mixing time $\dfrac{H^2}{\pi^2 K_z}$ (Okubo and Carter, 1966), the distribution becomes

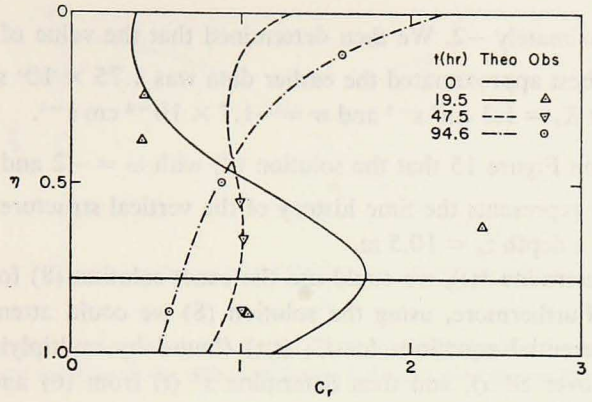

Figure 15. Observed values and theoretical curves for relative concentration C_r versus normalized depth $\eta = z/H$.

$$C_0(\infty,z) = \frac{Q}{H}\frac{\omega}{e^{\omega}-1} \quad e^{\omega \frac{z}{H}}. \tag{9}$$

Thus, if there is a net upward flow, the material which was initially concentrated in the vicinity of z_0 will eventually distribute exponentially with depth with higher concentrations in the upper layers.

In Figure 15 we have presented a comparison of theoretical curves of $C_0(t,z)/\frac{Q}{H}$ from (8), and data from Figures 14a, 14b, and 14d. The data represent the structure in the central and deepest part of the cross section. They are presented as relative concentrations C_r, found by dividing the concentration at any depth by the depth-mean concentration.

In evaluating the solution (8), the characteristic depth H was taken to be 15 m. We varied the other two parameters $\omega = \frac{wH}{K_z}$ and $\frac{H^2}{\pi^2 K_z}$ in order to best represent the data, but we did this in light of values obtained for w and K_z in the James River Estuary where hydrologic conditions are similar to those of the York. Pritchard (1954) estimated the mean upward directed vertical velocity in the James River from considerations of salt and volume continuity. He calculated vertical velocities of the order 1×10^{-3} cm s^{-1}. The results of Kent and Pritchard (1959) for the vertical diffusion of salt in the James suggest that vertical mean values for K_z should range from 0.5 to 5 cm^2 s^{-1}. If we assume that K_z is of order 1 cm^2 s^{-1}, then the vertical mixing time is of the order 2 days. The data from Figure 14d which represent the situation approximately 4 days after the release should approximate the distribution (9) for a proper choice of ω. In this way we determined that ω

should be approximately -2. We then determined that the value of $\frac{H^2}{\pi^2 K_z}$ for which the solution (8) best approximated the earlier data was 1.75×10^5 s; for $H = 15$ m this requires that $K_z = 1.3$ cm^2 s^{-1} and $w = -1.7 \times 10^{-3}$ cm s^{-1}.

It appears from Figure 15 that the solution (8) with $\omega = -2$ and $\frac{H^2}{\pi^2 K_z} = 1.75 \times 10^5$ s adequately represents the time history of the vertical structure of material initially released at a depth $z_0 = 10.5$ m.

In order to determine $\bar{x}(t)$, we could use the exact solution (8) for $C_0\ (t,z)$ in the expression (5). Furthermore, using the solution (8) we could attempt to solve the appropriate differential equations for $C_1\ (t,z)$ (found by multiplying (1)-(3) by x and integrating over all x), and then determine $\overline{x^2}\ (t)$ from (6) and finally $\sigma_x^2\ (t)$ from (7). The mathematical procedures involved would be somewhat complicated and the solutions would be very inconvenient for describing the behavior of $\bar{x}\ (t)$ and $\sigma_x^2\ (t)$ with time. Instead, we shall discuss the behavior of $\bar{x}\ (t)$ and $\sigma_x^2\ (t)$ for both small and large times directly from the moment equations.

Consider first the situation for very small times so that t is much less than the vertical mixing time. For these small times, with the exception of the case where the source is at the very surface or very bottom, boundary effects have not yet become important. We may, therefore, solve the moment equations for C_0 and C_1 for the case of an infinite extent in the vertical direction. From the moment equation for $C_0\ (t,z)$ and the relation (5) it can be shown that

$$\bar{x}\ (t) = v_1\left(1 - \frac{z_0}{d}\right)t + v_2\left(1 - \frac{z_0}{h}\right)\frac{1-\cos\sigma t}{\sigma} - v_1\frac{wt^2}{2d} + v_2\frac{wt\cos\sigma t}{h\sigma}$$

$$- v_2\frac{w\sin\sigma t}{h\sigma^2} = v_1\left(1 - \frac{z_0}{d}\right)t + \mathrm{O}\ (t^2)\,. \tag{10}$$

Similarly, from the moment equations for $C_1\ (t,z)$ and the relation (6) for $\overline{x^2}\ (t)$, we have for $\sigma_x^2\ (t)$ for very small times:

$$\sigma_x^2\ (t) = 2K_x t + \frac{2}{3}\left[\frac{v_1}{d}\right]^2 K_z t^3 + \mathrm{O}\ (t^4)\,. \tag{11}$$

The second term in this expression for variance represents the combined effect of the vertical shear in nontidal flow and vertical turbulent mixing (Okubo, 1967). Shear effect associated with the tidal current is not yet of importance. This is true in our case only because the time of release corresponded to a tidal slack.

Now consider the behavior of $\bar{x}\ (t)$ and $\sigma_x^2\ (t)$ for times very much greater than the vertical mixing time. The behavior of $\bar{x}\ (t)$ is found by substituting the asymptotic solution for C_0 (9) into the relation (5) to obtain

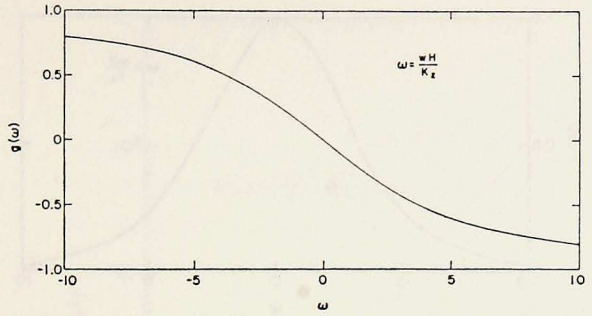

Figure 16. The function $g(\omega)$ representing the effect of vertical advection within the estuary on the longitudinal velocity of the center of mass of the dye distribution (see text).

$$\bar{x}(t) = \left\{ v_1 \left(1 - \frac{H}{2d} \right) + \left(\frac{2}{\omega} - \frac{e^{\omega}+1}{e^{\omega}-1} \right) v_1 \frac{H}{2d} \right\} t + \left\{ v_2 \left(1 - \frac{H}{2h} \right) + \left(\frac{2}{\omega} - \frac{e^{\omega}+1}{e^{\omega}-1} \right) \frac{v_2 H}{2h} \right\} \frac{1-\cos\sigma t}{\sigma} .$$

If t is also much larger than the tidal period this becomes

$$\bar{x}(t) = \left\{ v_1 \left(1 - \frac{H}{2d} \right) + \left(\frac{2}{\omega} - \frac{e^{\omega}+1}{e^{\omega}-1} \right) v_1 \frac{H}{2d} \right\} t$$

$$= \left\{ v_1 \left(1 - \frac{H}{2d} \right) + g(\omega)\, v_1 \frac{H}{2d} \right\} t . \qquad (12)$$

The first term on the right side of (12) is the depth-mean horizontal velocity, and the second term involving $g(\omega)$ represents a correction due to the presence of vertical velocity. The function $g(\omega)$ is plotted in Figure 16; its interpretation is quite simple. For $\omega = 0$, the correction term vanishes. For $\omega \to -\infty$, $\bar{x}(t) \to v_1 t$ because all the material has gathered at the surface, and for $\omega \to +\infty$ $\bar{x}(t) \to v_1 \left(1 - \frac{H}{d} \right) t$ because all the material has gathered at the bottom. For any values of $\omega < 0$, the asymptotic velocity of the patch will be greater than the mean velocity of the water column.

The procedures required to determine $\sigma_x^2(t)$ for large times are somewhat more involved. We first substitute the asymptotic solution for C_0 (9) into the moment equation for C_1, and then calculate $\overline{x^2}$ from (6) and finally σ_x^2. We will consider the two specific cases for which the time of vertical mixing is either much larger or much shorter than the tidal period. Remember that in either case the time t is much larger than the time for vertical mixing.

For the first case in which $\frac{H^2}{\pi^2 K_z} >> \frac{T}{\pi^2}$, we find (Okubo, 1968) for the asymptotic behavior of $\sigma_x^2(t)$:

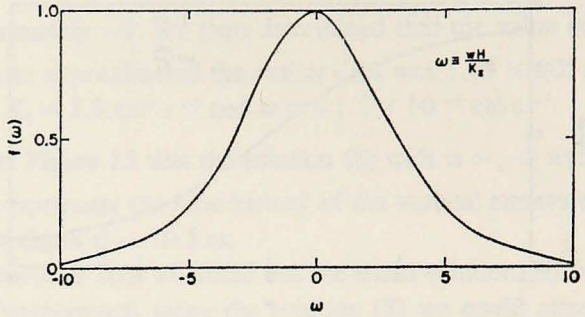

Figure 17. The function $f(\omega)$ representing the effect of vertical advection within the estuary on the asymptotic behavior of $\sigma_x^2(t)$ (see text).

$$\sigma_x^2(t) = 2K_x t + \frac{v_1^2 H^4}{60 K_z d^2} f(\omega) \left\{ 1 + O\left[\frac{v_2^2 T^2}{v_1^2 t_1^2} \right] \right\} t, \tag{13}$$

where t_1 is the time of vertical mixing and

$$f(\omega) = \frac{240}{\omega^4} \left\{ 1 - \frac{\omega^3 e^\omega (e^\omega + 1)}{2(e^\omega - 1)^3} \right\}. \tag{14}$$

The result (13) indicates that the shear effect due to the tidal current is negligible if the time required for the material to mix vertically is long compared with the tidal period. The second term on the right side of (13) represents only the shear effect associated with the nontidal current. The function $f(\omega)$ denotes a correction factor due to vertical advection; it is plotted in Figure (17). For $\omega = 0$, $f(\omega) = 1$ and there is no correction. For very large or small values of ω, $f(\omega) \to 0$; all of the material gathers either at the bottom or at the surface and there is no shear effect.

For the second case in which $\frac{H^2}{\pi^2 K_z} << \frac{T}{\pi^2}$, we find that the asymptotic behavior of $\sigma_x^2(t)$ is

$$\sigma_x^2(t) = 2K_x t + \frac{v_1^2 H^4}{60 K_z d^2} f(\omega)\, t + \frac{v_2^2 H^4}{118 K_z h^2} q(\omega)\, t. \tag{15}$$

The third term on the right represents the shear effect due to the tidal current; it is of importance in this case in which the time required for a material to mix vertically is short compared to the tidal period. The function $q(\omega)$ represents the correction in the tidal current shear effect due to vertical advection. It is an everywhere positive function. For $\omega = 0$, $q(\omega) = 1$; for large and small values of ω, $q(\omega) \to 0$. From (15) we see that the relative importance of the shear effect due to tidal and nontidal currents is proportional to the ratio of the square of surface current velocities. Therefore, if as in this case $\frac{H^2}{\pi^2 K_z} << \frac{T}{\pi^2}$, tidal currents can play a predominant role in the shear effect.

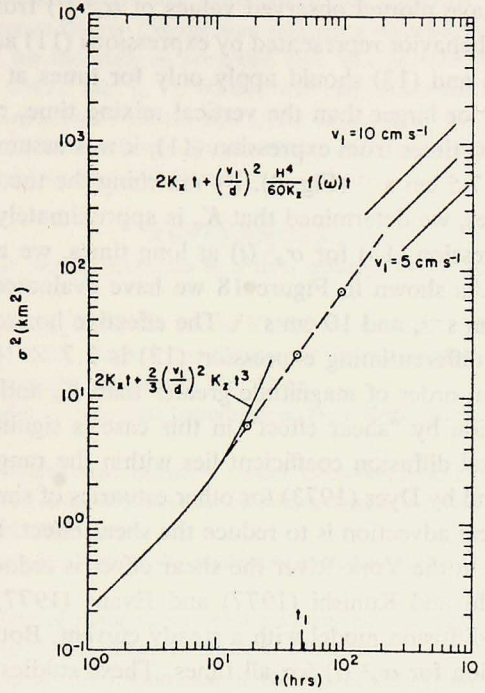

Figure 18. Comparison of observed values of σ_x^2 from Table 1. (data points) with asymptotic behavior predicted for times much shorter and much longer than the vertical mixing time $t_1 = \frac{H^2}{\pi^2 K_z}$.

4. Discussion

We have presented a model for longitudinal dispersion in a stratified estuary due to horizontal turbulence and to the interaction of vertical shear in both the tidal and nontidal currents with vertical mixing. Also included is the modification of these shear effects by nontidal upward advection. The expressions (11), (13) and (15) describe the asymptotic behavior of longitudinal variance determined from this model for times both very short and very long compared to the time of vertical mixing.

This predicted behavior may be compared with the values for longitudinal variance computed from the dye distribution (Table 1). By comparing the theoretical curves for C_0 (t,z) (the total amount of material per unit depth), we determined that $\omega = -2$, $w = -1.7 \times 10^{-3}$ cm s^{-1}, $K_z = 1.3$ cm^2 s^{-1}, and $\frac{H^2}{\pi^2 K_z} = 1.8 \times 10^5$s. This suggests that the vertical mixing time is long compared to $\frac{T}{\pi^2}$ (T is the semidiurnal tidal period) and that expression (13) rather than (15) for σ_x^2 (t) is appropriate to describe the variance at long times.

In Figure 18 we have plotted observed values of σ_x^2 (t) from Table 1 and indicated the asymptotic behavior represented by expressions (11) and (13). We assumed that expressions (11) and (13) should apply only for times at least one half order of magnitude smaller or larger than the vertical mixing time, respectively. In computing σ_x^2 (t) for short times from expression (11), it was assumed that $d = H/2 = 7.5$ m and that $v_1 = 7.5$ cm s^{-1} (Fig. 3). By matching the theoretical and observed variance at short times, we determined that K_x is approximately 2.8×10^5 cm^2 s^{-1}.

In evaluating expression (13) for σ_x^2 (t) at long times, we assumed that K_x was 2.8×10^5 cm^2 s^{-1}. As shown in Figure 18 we have evaluated this expression for $v_1 = 5$ cm s^{-1}, 7.5 cm s^{-1}, and 10 cm s^{-1}. The effective horizontal diffusion coefficient determined by differentiating expression (13) is 2.7×10^6 cm^2 s^{-1} for $v_1 = 7.5$ cm s^{-1}. This is an order of magnitude greater than K_x and so the enhancement of horizontal dispersion by "shear effect" in this case is significant. This value for the effective horizontal diffusion coefficient lies within the range of values reported by Bowden (1963) and by Dyer (1973) for other estuaries of similar nature.

The effect of vertical advection is to reduce the shear effect. For $\omega = -2$, $f(\omega) \cong 0.6$ (Fig. 17), and so in the York River the shear effect is reduced considerably.

Recently Oonishi and Kunishi (1977) and Evans (1977) have studied theoretically a two-layer diffusion model with a steady current. Both investigations have obtained the expression for σ_x^2 (t) for all times. These studies are both useful and encouraging. We have, however, had the advantage of working with a continuous shear model with both steady and oscillating currents. This has enabled us to discuss the vertical distribution of a tracer material with time as well as the behavior of moments of the distribution for both small and large times. The disadvantages of knowing only the asymptotic behavior of σ_x^2 (t) are, of course, obvious.

Both Oonishi and Kunishi and Evans have commented on the time periods of validity of the asymptotic formulas for σ_x^2 (t). For a vertical exchange time $\frac{H^2}{4K_z} = 72$ hours, Evans determined that the approximation for long times which varies linearly with time t might not be 90% accurate until after approximately one month (one month = 720 hours = $10\left(\frac{H^2}{4K_z}\right)$), and that his approximation for short times which depends on t^3 is 90% accurate only up to 4 hours after the beginning of the diffusion process. For our case we estimate a vertical exchange time of 20 hours, and so we might expect our approximation for long times to be valid after $10\left(\frac{H^2}{4K_z}\right) = 200$ hours. This does, in fact, compare favorably with our estimate for the period of validity for expression (13) as shown in Figure 18. Our estimate for the period of validity for expression (11) is not directly comparable with Evans' results because for very short times expression (11) varies linearly with t rather than as t^3.

Acknowledgments. Field work and some of the initial data reduction under this project were supported by the U.S. Atomic Energy Commission through a contract with the Chesapeake Bay Institute. Partial support for the analyses presented here was provided by the U.S. Geological Survey under Grant ER 08812. Mr. R. C. Whaley was responsible for conducting the difficult and involved field work associated with the dye tracer experiment. We gratefully acknowledge the generosity of Dr. D. W. Pritchard who supplied these data to us. This paper is Contribution No. 218 of the Marine Sciences Research Center.

REFERENCES

Bowden, K. F. 1963. The mixing processes in a tidal estuary, Int. J. Air Water Poll., *7*, 343–356.

—— 1965. Horizontal mixing in the sea due to a shearing current, J. Fluid Mech., *21*, 83–95.

Chesapeake Bay Institute 1957. York River Cruise: 29 July-1 August 1954. Data Report 30. The Johns Hopkins University, Baltimore, Md, 32 pp.

Dyer, K. R. 1973. Estuaries: A Physical Introduction. New York, John Wiley & Sons, 140 pp., (Table 5.5).

Evans, G. T. 1977. A two-layer shear diffusion model, Deep-Sea Res., *24*, 931–936.

Kent, R. E. and D. W. Pritchard. 1959. A test of mixing length theories in a coastal plain estuary, J. Mar. Res., *18*, 62–72.

Kent, R. E. 1960. Diffusion in a sectionally homogeneous estuary, Proc. Amer. Soc. Civil Engr., *86*, SA 2, 15–47.

Okubo, A. 1967. The effect of shear in an oscillatory current on horizontal diffusion from an instantaneous source, Int. J. Oceanogr. Limnol., *1*, 194–204.

—— 1968. Some remarks on the importance of the "shear effect" on horizontal diffusion, J. Oceanogr. Soc. Japan, *24*, 20–29.

Okubo, A. and H. H. Carter. 1966. An extremely simplified model of the "shear effect" on horizontal mixing in a bounded sea, J. Geophys. Res., *71*, 5267–5270.

Oonishi, Y. and H. Kunishi. 1977. On the coefficient of shear diffusion—its time dependence, J. Oceanogr. Soc. Japan, *33*, 165–167.

Pritchard, D. W. 1954. A study of the salt balance in a coastal plain estuary, J. Mar. Res., *13*, 133–144.

—— 1955. Estuarine circulation patterns, Proc. Amer. Soc. Civil Engr., *81*, No. 717.

Received: *19 January, 1978;* revised: *1 April, 1978.*